

Optimization of dual electrolyte and characteristic of micro-arc oxidation coating fabricated on ZK60 Mg alloy

LU Sheng¹, WANG Ze-xin¹, CHEN Jing², ZHOU Xiao-song¹

1. School of Materials Science and Engineering,

Jiangsu University of Science and Technology, Zhenjiang 212003, China;

2. School of Mechanical Engineering, Jiangsu University of Science and Technology, Zhenjiang 212003, China

Received 25 September 2010; accepted 20 December 2010

Abstract: Micro-arc oxidation (MAO) process was carried out in a dual electrolyte system of NaAlO_2 and Na_3PO_4 to develop compact, smooth and corrosion-resistant coatings on ZK60 Mg alloy by single factor experiments. The microstructural characteristics of coatings were investigated by X-ray diffractometry (XRD) and scanning electron microscopy (SEM) coupled with energy dispersive X-ray spectroscopy (EDS). Test of mass loss was conducted at a 3.5% NaCl solution to assess the resistance to corrosion. The effect of every element in the dual electrolyte system on voltage—time responses during MAO process and the coating characteristic were also analyzed and discussed systematically via single factor experiments. The results reveal that the main components of NaAlO_2 and Na_3PO_4 as well as additives of NaOH, NaB_4O_7 and $\text{C}_6\text{H}_5\text{Na}_3\text{O}_7$ demonstrate different effects on MAO process and coating characteristics. By means of single factor experiments, an optimized dual electrolyte system was developed, containing 17.5 g/L NaAlO_2 , 5.0 g/L Na_3PO_4 , 5.0 g/L NaOH, 3.0 g/L NaB_4O_7 and 4.2 g/L $\text{C}_6\text{H}_5\text{Na}_3\text{O}_7$.

Key words: magnesium alloy; micro-arc oxidation; dual electrolyte; optimization; single factor experiment

1 Introduction

Because of abundant reserves, low density and superior mechanical properties, Mg and its alloys offer various possibilities as regards applications in automobiles and airplanes to make them more fuel-efficient[1–2]. However, the practical applications of Mg alloys have been limited, which is mainly resulted from susceptibility to corrosion and wear[3]. It is significant to provide a coating to protect the magnesium alloys from corrosion.

Up to now, a lot of surface modification techniques have been developed for the protection of Mg alloys, among which micro-arc oxidization (MAO), also called plasma electrolytic oxidation (PEO), or anode spark deposition (ASD), based on conversional anodic oxidization technology, is a new promising surface treatment method of forming ceramic coatings on Al, Ti, Mg and their alloys. The surface properties, such as wear and corrosion resistance, electrical insulation,

microhardness, adhesion to substrate, can be considerably improved by MAO[4–6].

It is well known that properties of coatings fabricated by MAO mainly depend on the nature of substrate metal, the type of power source, the applied current density, the composition and concentration of electrolyte, etc[7–9]. Among all the parameters, the composition of electrolyte acts as the most important factor because of the incorporation of electrolyte elements into the anodic substrate in the oxidation[10]. Due to severe pollution to environment, acidic electrolyte system is seldom adopted in MAO process. Alkaline electrolyte system, mainly including aluminate, silicate and phosphate, is now widely used in MAO. In most cases, one of aluminate, silicate, and phosphate is selected as the main composition, plus borate, NaOH, fluoride and other additives, to produce the desired ceramic coatings[10–14].

It is supposed that mixture of more than one electrolyte will improve the microstructure and performance of MAO coatings. But a systematic research

of the effect of dual or multiple electrolytes has not been well documented in literatures. In the present work, aluminate (NaAlO_2) and phosphate (Na_3PO_4) were taken into account to form a dual electrolytes system with additives of NaB_4O_7 , NaOH and $\text{C}_6\text{H}_5\text{Na}_3\text{O}_7$ to develop compact, smooth and corrosion-resistant coatings on ZK60 Mg alloy under constant current mode. The aim is to study the effects of concentrations of every electrolyte and additive on voltage—time curves during MAO, microstructural characteristics and corrosion resistance, thus optimize the dual electrolyte system by means of single factor experiments.

2 Experimental

Rectangular coupons ($25\text{ mm} \times 25\text{ mm} \times 5\text{ mm}$) of ZK60 magnesium alloy (Zn 5.2%, Zr 0.47%, impurities $\leq 0.30\%$, Mg balance, mass fraction) were prepared by means of wire cut electrical discharge machining (WEDM) and polished with alumina waterproof abrasive paper up to 800 grits. And then the coupons were cleaned in an ultrasonic bath with acetone and ethyl alcohol, respectively, at room temperature for 10 min prior to MAO.

WHD-20 MAO system was employed and the experiments were carried out under constant current mode by controlling the voltage amplitude with current density of 30 A/dm^2 , frequency of 600 Hz, duty cycle of 40%. All MAO experiments were conducted at an electrolyte temperature of less than $35\text{ }^\circ\text{C}$ for 15 min and the voltage—time curves were recorded automatically in personal computer during MAO process.

The dual electrolyte system was prepared from distilled water containing 15–22.5 g/L NaAlO_2 , 2.5–7.5 g/L Na_3PO_4 , 3–6 g/L NaOH , 2–3.5 g/L NaB_4O_7 , and 2–3.5 g/L $\text{C}_6\text{H}_5\text{Na}_3\text{O}_7$. Single factor experiments were conducted in turn in the order of NaAlO_2 , Na_3PO_4 , NaOH , NaB_4O_7 , and $\text{C}_6\text{H}_5\text{Na}_3\text{O}_7$. From a single factor experiment, an optimized concentration of electrolyte or additive was selected based on the principle of corrosion resistance first, which became a constant parameter in the next single factor experiments.

The microstructural characteristics of coating, coating thickness and phase constituent were investigated by JSM-6480 SEM and Shimadzu XRD-6000. Test of mass loss was conducted at a 3.5% NaCl solution to assess the resistance of coating to corrosion.

3 Results and discussion

3.1 Coating evolution with NaAlO_2 concentration

As one of the main compositions of electrolyte, NaAlO_2 was selected as the variable with four

concentrations of 15.0, 17.5, 20.0 and 22.5 g/L in the first round single factor experiment where the aqueous solution consisted of other agents of 7.5 g/L Na_3PO_4 , 5.0 g/L NaOH , 3.0 g/L NaB_4O_7 and 3.6 g/L $\text{C}_6\text{H}_5\text{Na}_3\text{O}_7$.

The voltage—time responses during MAO with various concentrations of NaAlO_2 are shown in Fig.1, which display four distinguishing stages. At the first stage, voltage increases linearly, indicating the formation of anodic oxidation, at which a very thin, dense, and insulation film forms and the linear increase of the resistance occurs. The second stage corresponds to the main period of MAO, which is known to involve a large number of short-lived sparks (electrical discharges), caused by localized electrical breakdown of the growing coating[4, 15]. The value of voltage increases up to 250–350 V with many severe discharge spots on the substrate surface. It is notable that tip discharges frequently appear at this stage for NaAlO_2 concentration of 15.0, 20.0 and 22.5 g/L, except 17.5 g/L. The third stage presents a sharp drop followed by the fourth stage, a plateau with voltage of around 160 V, in which many tiny and dense sparks are formed on the substrate.

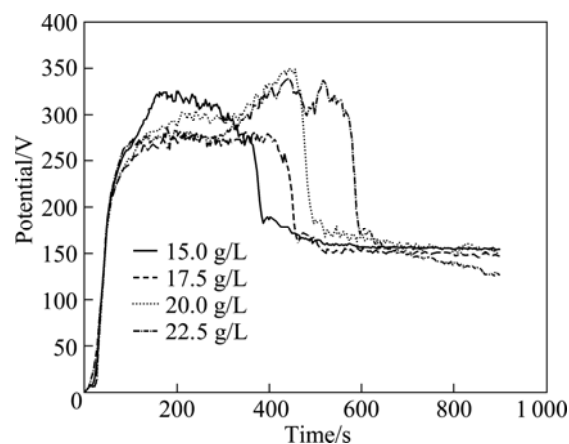


Fig.1 Voltage—time curves with various concentrations of NaAlO_2 during MAO

The corrosion rate and thickness of coating with various concentrations of NaAlO_2 are shown in Fig.2. It is found that the lowest corrosion rate is $0.1348\text{ g/(m}^2\cdot\text{h)}$ (17.5 g/L NaAlO_2) with coating thickness of $72\text{ }\mu\text{m}$, while the highest corrosion rate is $0.89\text{ g/(m}^2\cdot\text{h)}$ (22.5 g/L NaAlO_2), which corresponds to the thinnest coating of $43\text{ }\mu\text{m}$. It is proved that coating thickness plays a key role in the corrosion resistance.

The result of XRD indicates that the coating mainly consists of MgAl_2O_4 and a small amount of MgO . Figure 3 shows surface morphology of MAO coatings with various concentrations of NaAlO_2 . With increase of NaAlO_2 concentration, the surface of the coatings becomes more compact and is characterized with large pores and micro-cracks. As shown in Fig.4, for 17.5 g/L

NaAlO₂ the coating of 72 μm is uniform with a loose outer layer and a dense internal layer which could prevent the substrate from corrosion. But for 22.5 g/L NaAlO₂, the coating is very uneven with the thinner part of only 19 μm and the thicker part of 92 μm. It can be considered that when the samples with thin and uneven MAO coating were immersed in an aggressive medium, corrosive atom could penetrate into the substrate easily through the thinner part of the coating, thus lead to serious corrosion. It also reveals that corrosion resistance of MAO coating is not only decided by the thickness, but also by the uniformity and compactness.

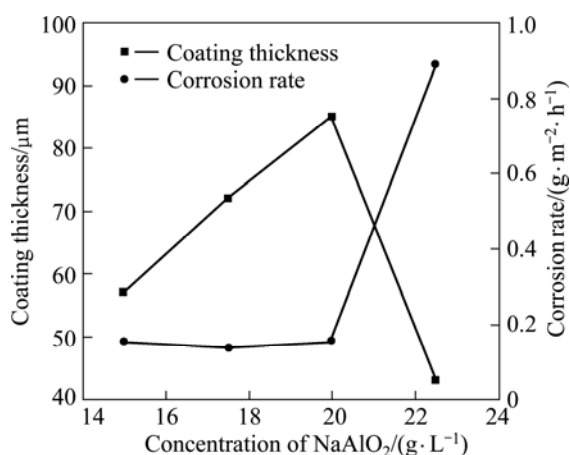


Fig.2 Thickness and corrosion rate with various concentrations of NaAlO₂

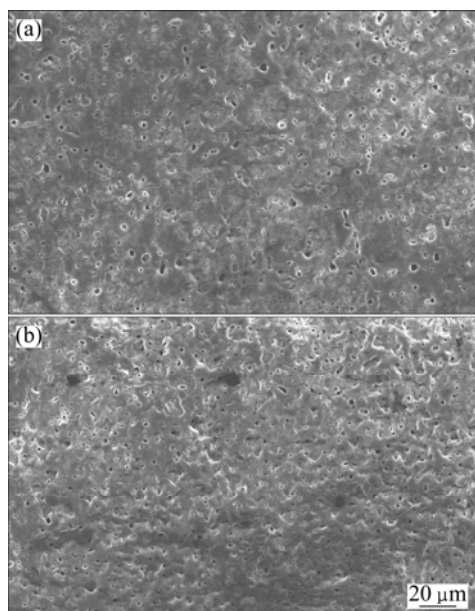


Fig.3 Surface morphologies of MAO coating with various concentrations of NaAlO₂: (a) 17.5 g/L; (b) 22.5 g/L

Furthermore, useful information could be drawn out from the voltage—time responses during MAO. The second stage of voltage—time curve mentioned above is very stable (around 270 V) for coating with 17.5 g/L

NaAlO₂, which corresponds to a thick, compact and even coating, enhancing corrosion resistance. But for coating with 22.5 g/L NaAlO₂, the second stage is very long (around 450 s) and fluctuant (from 280 to 340 V), which results in an uneven coating with weak corrosion resistance.

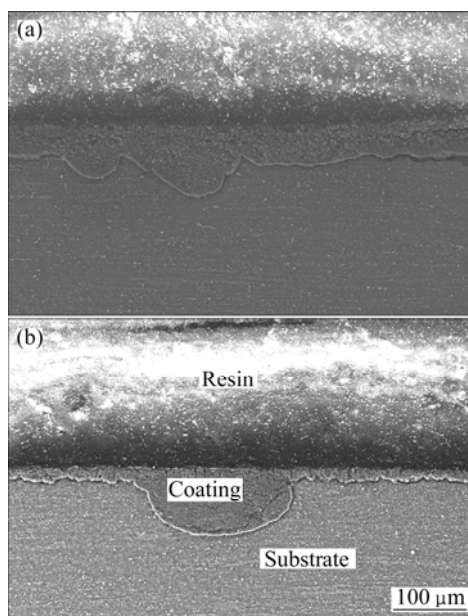


Fig.4 Cross-section morphologies of MAO coating with various concentrations of NaAlO₂: (a) 17.5 g/L; (b) 22.5 g/L

From the analysis above, morphology and corrosion resistance of the coating with 17.5 g/L NaAlO₂ are better, 17.5 g/L is regarded as the optimized NaAlO₂ concentration for the next signal factor experiments.

3.2 Coating evolution with Na₃PO₄ concentration

Acted as the other main compositions to form the MAO coating, Na₃PO₄ was arranged to be optimized in the second single factor experiment from four concentrations of 2.5, 5.0, 7.5 and 10 g/L. Other elements of the MAO solution were 17.5 g/L NaAlO₂, 3.6 g/L NaOH, 3.0 g/L NaB₄O₇ and 3.6 g/L C₆H₅Na₃O₇, respectively.

It can be seen from Fig.5 that with increase of Na₃PO₄ concentration (from 2.5 g/L to 10.0 g/L), the voltage—time responses become smoother and their peak values tend to decrease. And all of the four voltage—time curves are more stable than those of the first experiment. This is due to the optimization of NaAlO₂, which helps to reduce the cases of tip discharge during the second stage (main MAO stage). Among them, 2.5 g/L Na₃PO₄ concentration is characterized with the highest peak, large fluctuant (from 270 to 370 V) and long second stage (around 560 s), while other three samples share the similar voltage—time curves with shorter (around 220 s) and smoother the second stage (from 270 to 300 V).

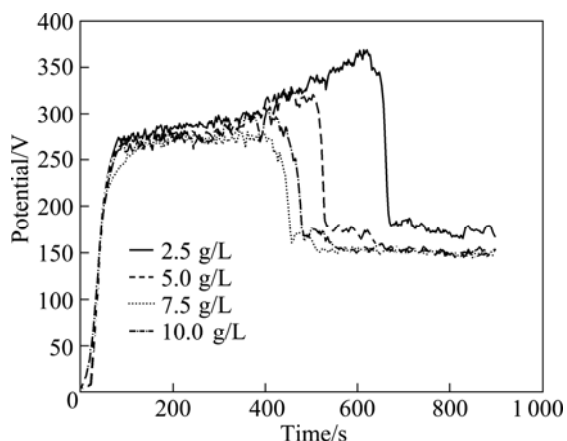


Fig.5 Voltage — time curves during MAO with various concentrations of Na_3PO_4

Figure 6 shows that the three coatings with Na_3PO_4 concentrations of 5.0, 7.5 and 10.0 g/L are characterized with thicker coating and higher corrosion resistance, among them coating with 5.0 g/L Na_3PO_4 is notable for the thickest (98 μm) and the lowest corrosion rate (0.036 8 $\text{g}/(\text{m}^2\cdot\text{h})$). In contrast, coating produced with 10.0 g/L Na_3PO_4 is thinner (50 μm) and higher corrosion rate (0.441 2 $\text{g}/(\text{m}^2\cdot\text{h})$) which is still better than that of the optimized coating (0.134 8 $\text{g}/(\text{m}^2\cdot\text{h})$) in the first factor experiment.

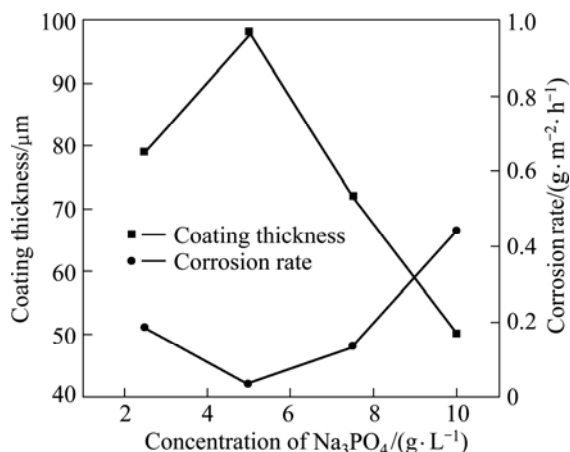


Fig.6 Thickness and corrosion rate with various concentrations of Na_3PO_4

The surface and the cross-section morphologies of the coating prepared with 5.0 g/L Na_3PO_4 are shown in Fig. 7. It is observed that the coating is more uniform and smoother with very tiny voids or pores and fewer micro-cracks compared with the coatings in the first round factor experiment. This accounts for better corrosion resistance.

Again decided by corrosion resistance, 5.0 g/L Na_3PO_4 is recognized as the optimized concentration for the next signal factor experiments.

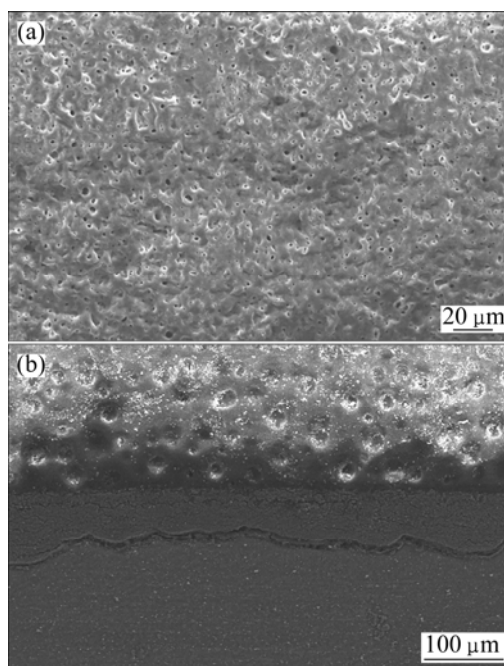


Fig.7 Morphologies of MAO coating with 5.0 g/L Na_3PO_4

3.3 Coating evolution with NaOH concentration

NaOH was added into the electrolyte solution to adjust the conductivity and pH value to ensure the solution weak alkaline[16]. In the third round single factor experiment, NaOH was the only variable with concentrations of 3.0, 4.0, 5.0 and 6.0 g/L, and the other elements of the MAO solution were 17.5 g/L NaAlO_2 , 5.0 g/L Na_3PO_4 , 3.0 g/L NaB_4O_7 and 3.6 g/L $\text{C}_6\text{H}_5\text{Na}_3\text{O}_7$.

Figure 8 represents the voltage—time responses during MAO with various concentrations of NaOH . There are also four stages but with large difference between each other when concentration of NaOH varies, owing to the enhanced conductivity. With increase of the NaOH concentration, both the peak value and period of the second stage decrease gradually. And the curves

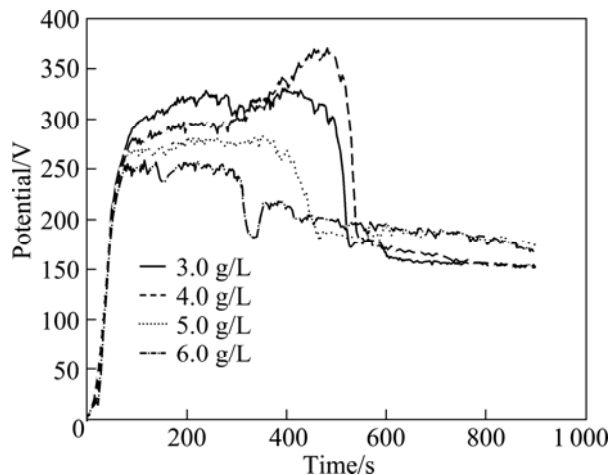


Fig.8 Voltage — time curves during MAO with various concentrations of NaOH

become smoother than those of the 1st and the 2nd round experiments. This illuminates that NaOH is an important additive to influence MAO process.

As shown in Fig.8 and Fig.9, the voltage—time curves are very smooth with lower peak value (260 V) and shorter period of the second stage (around 300 s) when 5 g/L NaOH was added, which results in a thick (98 μm) and good corrosion-resistant (0.0368 g/(m²·h)) coating. It is noticed that this optimized sample is the same one optimized in the second signal factor experiment. And the NaOH concentration of 5.0 g/L is considered the optimized for the next signal factor experiments.

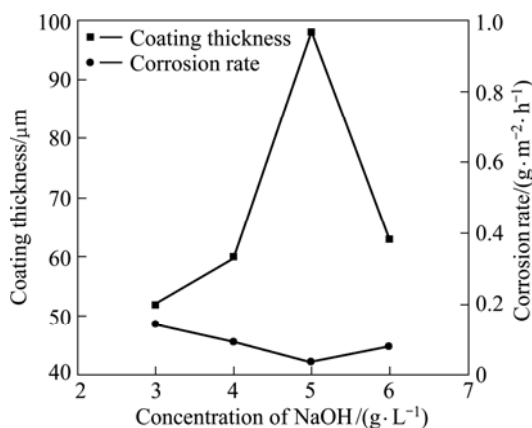


Fig.9 Thickness and corrosion rate with various concentrations of NaOH

3.4 Coating evolution with NaB₄O₇ concentration

The important effects of NaB₄O₇ on the thickness and wear resistance of coating were reported in Ref.[17]. In the fourth single factor experiment, NaB₄O₇ was added into the electrolyte solution as the variable with concentrations of 2.0, 2.5, 3.0 and 3.5 g/L, respectively, while the other elements of the MAO solution were 17.5 g/L NaAlO₂, 5.0 g/L Na₃PO₄, 5.0 g/L NaOH and 3.6 g/L C₆H₅Na₃O₇, respectively.

The voltage—time responses during MAO are illustrated in Fig.10 with various concentrations of NaB₄O₇. It is obvious that NaB₄O₇ has a remarkable effect on the MAO process. The voltage peak value decreases evidently to only 270 V for all the four samples and the period of the 2nd stage lasts only around 200 s, which make a great difference from the former three experiments. All the four samples here represent good corrosion resistance (from 0.0724 to 0.0368 g/(m²·h)). Among them, the sample produced with 3.0 g/L NaB₄O₇ corresponds to the optimized sample in the 3rd round experiment and also exhibits the best corrosion resistance (0.0368 g/(m²·h)) with the thickest coating (98 μm), as seen in Fig.11. Therefore, 3.0 g/L was taken for the optimized concentration of NaB₄O₇ for the final signal factor experiment.

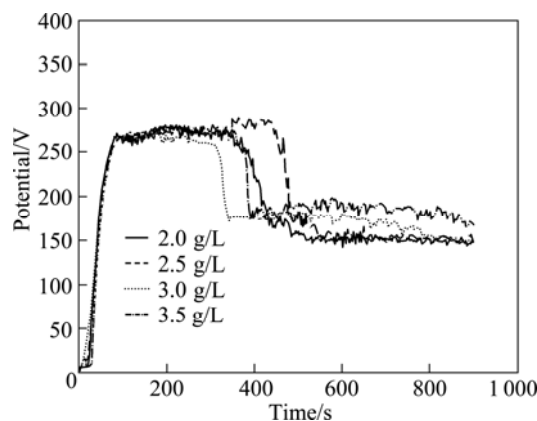


Fig.10 Voltage—time curves during MAO with various concentrations of NaB₄O₇

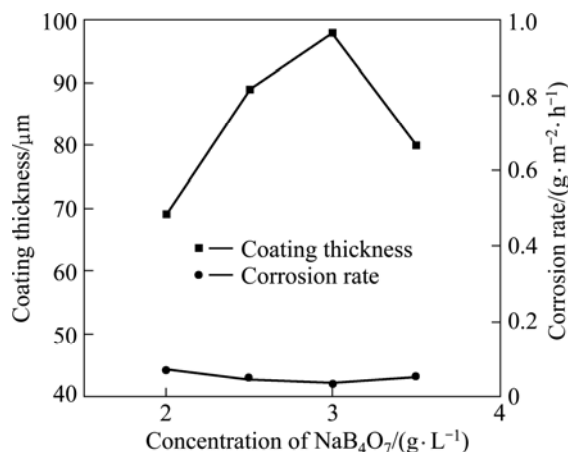


Fig.11 Thickness and corrosion rate with various concentrations of NaB₄O₇

3.5 Coating evolution with C₆H₅Na₃O₇ concentration

In the final single factor experiment, C₆H₅Na₃O₇ was selected as an additive into the electrolyte solution for the only variable concentrations of 2.0, 2.5, 3.0 and 3.5 g/L, respectively, while the rest elements of the MAO solution were 17.5 g/L NaAlO₂, 5.0 g/L Na₃PO₄, 5.0 g/L NaOH and 3.0 g/L NaB₄O₇, respectively.

C₆H₅Na₃O₇ was used as an additive with the function of restraining spark. From Fig.12, it is easy to find that the voltage—time responses during MAO with various concentrations of C₆H₅Na₃O₇ present perfect smoothness with the voltage fluctuated around 260 V and the period of the 2nd stage around 180 s. This indicates that C₆H₅Na₃O₇ has the ability to prevent the MAO process from tip discharge. All the samples fabricated in this round experiment are characterized with lower corrosion resistance (from 0.038 4 to 0.025 6 g/(m²·h)). Among them, coating produced with 4.2 g/L C₆H₅Na₃O₇ exhibits the best corrosion-resistant (0.0256 g/m²h), as shown in Fig.13, while its thickness is only 70 μm.

Figure 14 shows the morphology of MAO coating with 4.2 g/L C₆H₅Na₃O₇. It is obvious that the coating is

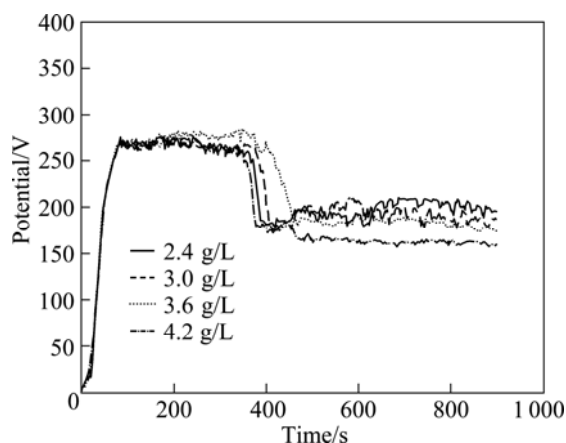


Fig.12 Voltage—time curves during MAO with various concentrations of $C_6H_5Na_3O_7$

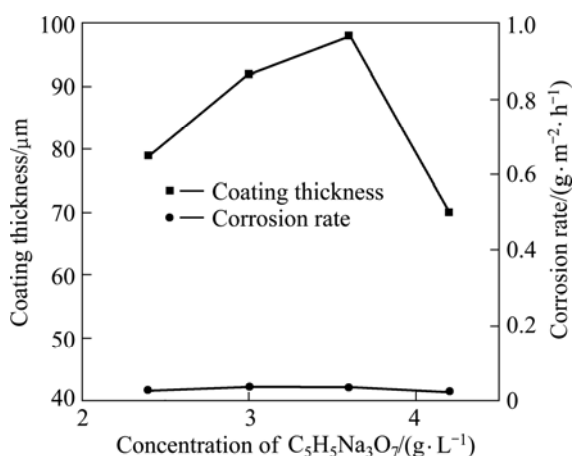


Fig.13 Thickness and corrosion rate with various concentrations of $C_6H_5Na_3O_7$

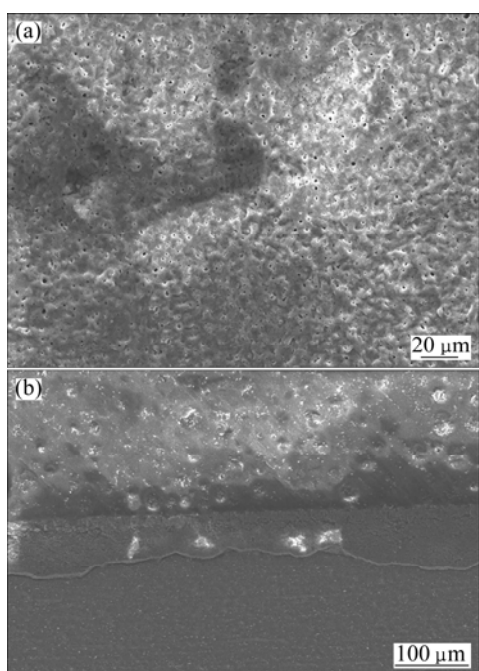


Fig.14 Morphologies of MAO coating with 4.2 g/L $C_6H_5Na_3O_7$

very smooth and compact with few pores and microcracks on the surface while its thickness is very uniform. This may contribute to the best corrosion resistance although with relatively thinner coating compared with others.

Therefore, according to the principle of corrosion resistance, an optimum composition of the dual electrolyte is as follows: 17.5 g/L $NaAlO_2$, 5.0 g/L Na_3PO_4 , 5.0 g/L $NaOH$, 3.0 g/L NaB_4O_7 and 4.2 g/L $C_6H_5Na_3O_7$, which was deduced by means of the five single factor experiments.

4 Conclusions

1) By means of single factor experiments, an optimized dual electrolyte system is developed, containing 17.5 g/L $NaAlO_2$, 5.0 g/L Na_3PO_4 , 5.0 g/L $NaOH$, 3.0 g/L NaB_4O_7 and 4.2 g/L $C_6H_5Na_3O_7$.

2) The coating prepared by the optimized dual electrolyte consists of $MgAl_2O_4$ and a small amount of MgO is characterized with compact, smooth, uniform and high corrosion resistance.

3) The concentrations of main compositions ($NaAlO_2$ and Na_3PO_4) and additives ($NaOH$, NaB_4O_7 and $C_6H_5Na_3O_7$) present different effects on the MAO process and coating quality. A relative short voltage—time response will help to produce a coating with good corrosion resistance.

4) The thickness, uniformity and compactness of the coating play significant roles in the corrosion resistance.

References

- [1] AGNEW S R. Wrought Magnesium: A 21st century outlook [J]. *Journal of the Minerals, Metals and Materials Society*, 2004, 56: 20–21.
- [2] KULEKCI M K. Magnesium and its alloys applications in automotive industry [J]. *The International Journal of Advanced Manufacturing Technology*, 2008, 39: 851–865.
- [3] GHALI E, DIETZEL W, KAINER K U. Testing of general and localized corrosion of magnesium alloys: A critical review [J]. *Journal of Materials Engineering and Performance*, 2004, 13: 517–529.
- [4] SU Pei-bo, WU Xiao-hong, GUO Yun, JIANG Zhao-hua. Effects of cathode current density on structure and corrosion resistance of plasma electrolytic oxidation coatings formed on ZK60 Mg alloy [J]. *Journal of Alloys and Compounds*, 2009, 475: 773–777.
- [5] GU Wei-chao, LÜ Guo-hua, CHEN Huan, CHEN Guang-liang, FENG Wen-ran, YANG Si-ze. PEO protective coatings on inner surface of tubes [J]. *Surface & Coatings Technology*, 2007, 201: 6619–6622.
- [6] PAITAL S R, DAHOTRE N B. Calcium phosphate coatings for bio-implant applications: Materials, performance factors, and methodologies [J]. *Materials Science and Engineering R*, 2009, 66: 1–70.
- [7] ARRABAL R, MATYKINA E, HASHIMOTO T, SKELDONAND P, THOMPSON G E. Characterization of AC PEO coatings on magnesium alloys [J]. *Surface & Coatings Technology*, 2009, 203:

- 2207–2220.
- [8] DUNLEAVY C S, GOLOSNOY I O, CURRAN J A, CLYNE T W. Characterisation of discharge events during plasma electrolytic oxidation [J]. *Surface & Coatings Technology*, 2009, 203: 3410–3419.
- [9] JIN F Y, CHU P K, XU G D, ZHAO J, TANG D L, TONG H H. Structure and mechanical properties of magnesium alloy treated by micro-arc discharge oxidation using direct current and high-frequency bipolar pulsing modes[J]. *Materials Science and Engineering A*, 2006, 435–436: 123–126.
- [10] LUO Hai-he, CAI Qi-zhou, WEI Bo-kang, YU Bo, LI Ding-jun, HE Jian, LIU Ze. Effect of $(\text{NaPO}_3)_6$ concentrations on corrosion resistance of plasma electrolytic oxidation coatings formed on AZ91D magnesium alloy [J]. *Journal of Alloys and Compounds*, 2008, 464: 537–543.
- [11] CHEN Fei, ZHOU Hai, YAO Bin, QIN Zhen, ZHANG Qing-feng. Corrosion resistance property of the ceramic coating obtained through microarc oxidation on the AZ31 magnesium alloy surfaces [J]. *Surface & Coatings Technology*, 2007, 201: 4905–4908.
- [12] SHANG Wei, CHEN Bai-zhen, SHI Xi-chang, CHEN Ya, XIAO Xiang. Electrochemical corrosion behavior of composite MAO/sol–gel coatings on magnesium alloy AZ91D using combined micro-arc oxidation and sol–gel technique [J]. *Journal of Alloys and Compounds*, 2008, 38: 541–545.
- [13] ZHANG Rong-fa, SHAN Da-yong, HAN En-hou, GUO Shi-bo. Development of microarc oxidation process to improve corrosion resistance on AZ91 HP magnesium alloy [J]. *Trans Nonferrous Met Soc China*, 2006, 16: s685–s688.
- [14] SHI Xing-ling, WANG Qing-liang, WANG Fu-shun, GE Shi-rong. Effects of electrolytic concentration on properties of micro-arc film on Ti6Al4V alloy [J]. *Mining Science and Technology*, 2009, 19: 220–224.
- [15] WANG Yan-hua, WANG Jia, ZHANG Ji-biao, ZHANG Zhan. Effects of spark discharge on the anodic coatings on magnesium alloy [J]. *Materials Letters*, 2006, 60: 474–478.
- [16] GUO H F, AN M Z, HUO H B, XU S, WU L J. Microstructure characteristic of ceramic coatings fabricated on magnesium alloys by micro-arc oxidation in alkaline silicate solutions [J]. *Applied Surface Science*, 2006, 252: 7911–7916.
- [17] YANG Guo-ying, ZHANG Ying. Study on additives in micro-arc oxidation process of magnesium alloy [J]. *Journal of Shaoxing University: Natural Science*, 2005, 25: 42–45. (in Chinese)

ZK60 镁合金微弧氧化双电解液的优化及膜层特性

芦 笙¹, 王泽鑫¹, 陈 静², 周小淞¹

1. 江苏科技大学 材料科学与工程学院, 镇江 212003; 2. 江苏科技大学 机械工程学院, 镇江 212003

摘 要: 在 NaAlO_2 和 Na_3PO_4 组成的双电解液体系中对 ZK60 镁合金进行微弧氧化处理, 通过单因素实验制备出致密、平整、耐腐蚀的涂层。采用 XRD、SEM 和 EDS 研究膜层的显微组织, 并在 3.5% NaCl 溶液中进行静态质量损失实验, 测试膜层的耐腐蚀性能。分析讨论电解液中各组元浓度对微弧氧化过程中电压—时间曲线和膜层特性的影响。结果表明: 主成膜剂 NaAlO_2 、 Na_3PO_4 及辅助添加剂 NaOH、 NaB_4O_7 和 $\text{C}_6\text{H}_5\text{Na}_3\text{O}_7$ 对微弧氧化过程和膜层特性有不同的影响, 单变量实验优化得到的双电解液成分为 17.5 g/L NaAlO_2 , 5 g/L Na_3PO_4 , 5 g/L NaOH, 3 g/L NaB_4O_7 和 4.2 g/L $\text{C}_6\text{H}_5\text{Na}_3\text{O}_7$ 。

关键词: 镁合金; 微弧氧化; 双电解液; 优化; 单因素实验

(Edited by LI Xiang-qun)